Measurements of the Hollow Beam at the Wake Field Transformer Experiment at DESY

F.-J. Decker, W. Bialowons, M. Bieler, H.-D. Bremer, H.-C. Lewin, P. Schütt*, G.-A. Voss, R. Wanzenberg, T. Weiland

Deutsches Elektronen-Synchrotron DESY, Notkestr. 85, 2000 Hamburg 52, Germany

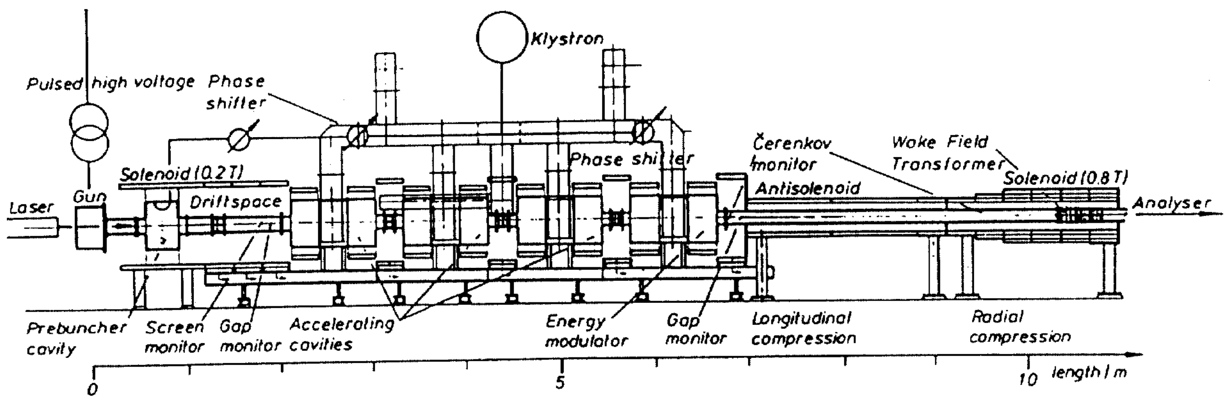

Figure 1: Overall layout of the Wake Field Transformer experiment at DESY.

Abstract

Future accelerator concepts, such as wake field accelerators, need drive beams with high current and short bunches in order to create a high accelerating gradient. Here, the investigations of the hollow drive beam for the *Wake Field Transformer* Experiment at DESY are presented. Besides the usual beam qualities, like high peak current and short bunch length, other parameters such as the azimuthal distribution and radial thickness of the hollow beam have to be observed. This is achieved with fluorescent screens and gap monitors. Space charge effects and the bunching mechanism in a prebuncher section can also be investigated. Shorter bunches at the end of the linac and especially behind a high energy buncher system have to be detected by a Čerenkov monitor in combination with a streak camera (resolution 5 ps).

1 Introduction

In order to accelerate a high energy beam, in many modern and future accelerators the energy is extracted from a low energy, high current drive beam. A promising new energy transfer mechanism is the transformation of wake fields by a special *Wake Field Transformer* [1,2]. The wake fields are excited by a hollow drive beam of high charge (1 μC) and are spatially focused to the centre. There, a second beam can be accelerated with a gradient of up to 200 MeV/m.

At DESY an experiment with a hollow beam wake field transformer has been set up [3,4,5]. It has demonstrated for the first time [6], that this mechanism works and also has pointed out the major technical difficulties. In a first "proof of principle" experiment quite long bunches (1 cm rms) with a charge of 0.1 μC have produced a measured accelerating gradient of 8 MeV/m.

The investigations and measurements of the hollow driving beam bunches are the main topic in this paper.

2 Experimental Set Up

The major components (see fig. 1) for creating, forming and accelerating hollow beam bunches are a laser driven gun, a prebuncher system, a linac consisting of four accelerating cavities, a beam guiding system by solenoids and a high energy buncher, where the relativistic bunches ($\approx$ 6.5 MeV) are longitudinally compressed before entering the *Wake Field Transformer*. The diagnostic elements for the hollow beam, especially fluorescent screens, gap monitors and Čerenkov monitors are mounted in the drift space behind the prebuncher cavity, at the end of the linac and behind the antisolenoid of the high energy buncher. The behavior of the hollow beam and its parameters have been investigated in detail with these monitors, which are briefly discribed below.

3 Diagnostic Equipment

Fluorescent Screen Monitor. Projections of the hollow beam are produced by fluorescent screens. They can be moved into the beam pipe and are observed by video cameras. Fig. 2 shows the hollow beam in the drift space before it enters the linac. The transverse position and the ring thickness is measurable within a resolution of $\pm$0.5 mm. The azimuthal homogeneity can only be estimated and must be quantitatively determined by a gap monitor.

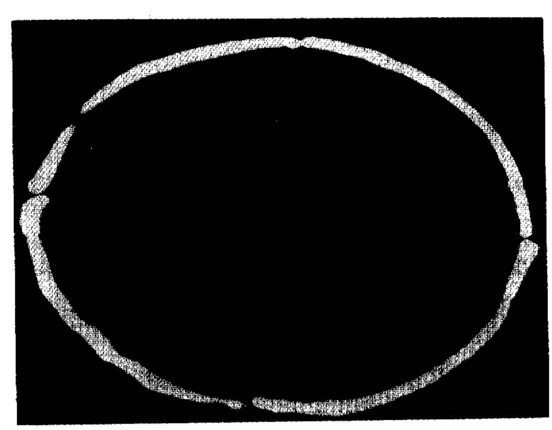

Figure 2: Image of the hollow beam.

*Now Department of Physics, University of Maryland, USA

Gap Monitor. The beam induces an image current on the wall of the pipe. This current and its distribution can be measured with a gap monitor. Therefore the pipe is interrupted by a ceramic ring, the gap, which is bridged by resistors. The voltage drops across these resistors are picked up by 50 Ω-cables around the circumference of the pipe. So the amplitude as well as the azimuthal and longitudinal distribution of the wall current can be determind.

The longitudinal resolution of the gap monitor is mainly limited by its resonance frequency $\omega = 1/\sqrt{LC}$, where C and L are determined by the geometry of the ceramic ring (capacitance of two plates, 1/2 of the inductance of a long coil):

$$C = \varepsilon\varepsilon_0 \frac{2\pi r h}{d} \quad \text{and} \quad L \approx \frac{1}{2}\mu\mu_0 \frac{dh}{2\pi r}.$$

With a mean radius $r = 58.5$ mm of the ceramic ring, a thickness $d = 4$ mm and a radial heigth $h = 7$ mm the capacitance is $C = 50$ pF ($\varepsilon = 8.8$) and $L = 50$ pH, so $\nu = \omega/2\pi = 3.2$ GHz. The shortest pulse length σ_{min} that can be resolved is about:

$$\sigma_{min} = \frac{1}{\omega} = \sqrt{LC} = \sqrt{\frac{\varepsilon}{2}\frac{h}{c}} \approx 50\,\text{ps}$$

for our device. To increase the resolution the height h must be decreased, but this would impair the mechanical stability.

Shorter bunches excite an oscillation of the gap monitor, if the total resistance R_z of the monitor is not adapted to dampen them. $R_z = \sqrt{L/C}$ near the aperiodic case $(2\sqrt{L/C})$ is the best choice to get the fastest response, a good damping of the oscillations and an acceptable estimation for the charge Q of a shorter pulse $Q \approx \hat{I}\Delta t$ ($\hat{I}$: peak current, Δt: FWHM).

The azimuthal resolution is in competition with the damping of longitudinal oscillations, because the time for an azimuthal cross talk between different pick ups is given by $t = L_\phi/R_z$ ($L_\phi \approx 2\mu_0 \cdot 2\pi r$). To increase this time and hence the resolution, R_z must be decreased to the smallest possible value at which the voltage drop for the expected wall current is still measurable.

For a given cross talk the measured data have to be corrected [7], to get the azimuthal distribution of the hollow beam. Fig. 3 shows a measured azimuthal voltage distribution for three different beam currents (8 A, 22 A, 33 A). The dipole moment of the fitted curve is about 10 % of the maximal possible moment corresponding to an offset of 5 mm of a perfectly symmetric bunch. The dip at pick-up no. 7 can also be found in fig. 2, where a lower intensity is in the upper left part of the ring.

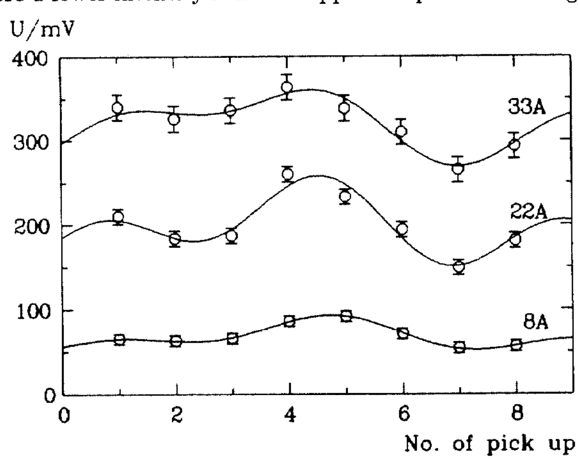

Figure 3: Azimuthal distribution of the hollow beam, measured by eight pick-ups around the circumference of the pipe.

Čerenkov Monitor. To overcome the longitudinal resolution limit of gap monitors a special monitor using Čerenkov radiation has been built. A part of the electron ring creates Čerenkov light in a quartz wedge. The light is guided by lenses and mirrors away from the solenoid field to the imaging slot of a streak camera. With this camera the time distribution of the incoming light and hence the longitudinal distribution of the hollow beam can be determined with a resolution of 5 ps (σ). The corresponding peak current must be derived from the pulse height of the gap monitor mounted nearby and the ratio of the measured bunch lengths: $\hat{I} \approx \hat{I}_{gap} \cdot \sigma_{gap}/\sigma_{Cer}$.

4 Results of Bunch Compression

Besides the radial thickness and the azimuthal distribution of the hollow beam, which are mentioned in connection with the description of the monitors, a short bunch length is important for the creation of strong wake fields.

Prebuncher. Fig. 4 shows the bunch compression behavior of two bunches ($E_{kin} = 80$ keV) for different peak currents, measured with a gap monitor at the end of the prebuncher drift space. At a low current ($I_0 = 3$ A), a short bunch length $\Delta t = 250$ ps (FWHM) is achieved. This induces the gap monitor oscillations, thus limiting the resolution. At a higher current ($I_0 = 50$ A) the longitudinal space charge suppresses a further bunch compression at this low energy.

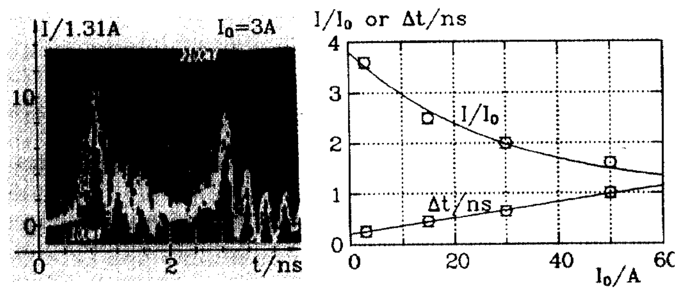

Figure 4: Bunch compression at the end of the drift space, left: monitor signal, right: achieved bunch length Δt (FWHM) and peak current increasement I/I_0 for different gun currents (I_0).

Linac. During the acceleration in the linac the bunch is furthe compressed. This can only be observed with the Čerenkov mon itor at the end of the linac. The shortest light signals of abou $\sigma = 10$ ps occur at low currents ($I_0 < 3$ A), while the longes signals with $\sigma \approx 80$ ps occur at higher currents ($I_0 > 30$ A) an reveal an intensity structure (Fig. 5). This can be explained b a radial structure of the bunch over its length. By properly ad justing the strength of the guiding solenoid field and the phase of the accelerating cavities, bunches with almost only one ligh pulse of $\sigma \approx 30$ ps can be achieved.

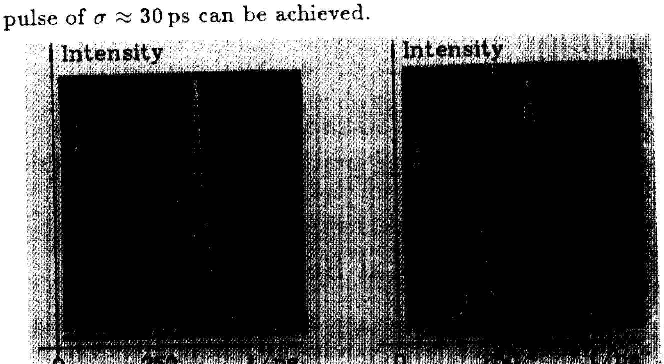

Figure 5: Bunch length at low (left) and high (right) current

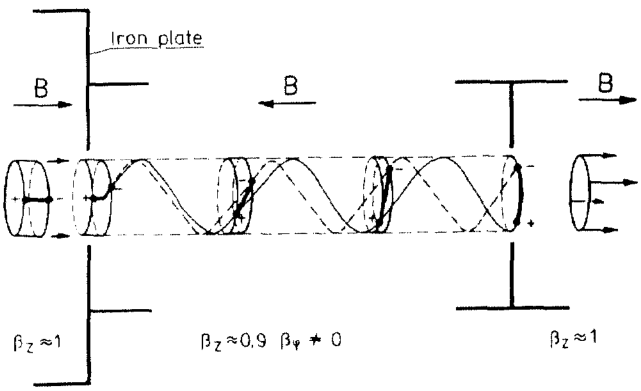

Figure 6: Bunching mechanism by hollow beam rotation.

High energy buncher. The final longitudinal compression of the hollow beam is achieved in the antisolenoid of the high energy buncher (compare fig. 1 and fig. 6). When the guiding magnetic field is reversed in the antisolenoid, the hollow beam experiences an azimuthal kick at the field concentrating iron plate and spirals around its axis of symmetry. The longitudinal velocity β_z decreases and a bunch compression is possible, if the phase of the fourth cavity is adjusted so that the earlier particles are accelerated less ("−") than the later ones ("+" in fig. 6). At the end of the antisolenoid, where the bunch is short, the rotation is stopped by a second inversion of the solenoid field. In addition to the compression, possible inhomogenieties are smeared out by the rotation.

The longitudinal compression is controlled by two Čerenkov monitors in front of and behind the antisolenoid. The Čerenkov light of the first monitor is optically delayed and combined with the second one, before they are guided to one streak camera. Figure 7 (left) shows three bunches before (1.) and after (2.) the rotation, simultaneously measured with the streak camera. The different light spots of "1." and "2." are visible at the top and the middle of the picture.

By measuring the time difference Δt of the second Čerenkov monitor signals with and without rotation the energy of the hollow beam can be determined by:

$$E = cBR\left(1-\left(\frac{L\beta}{L+c\Delta t}\right)^2\right)^{-1/2},$$

where B is the magnetic field strength, R the hollow beam radius, L the length of the antisolenoid section and β the velocity before the rotation. $E = (6.5 \pm 0.3)\,\mathrm{MeV}$ has been measured, where the error limits mainly depend on the limits of B and R and not of Δt.

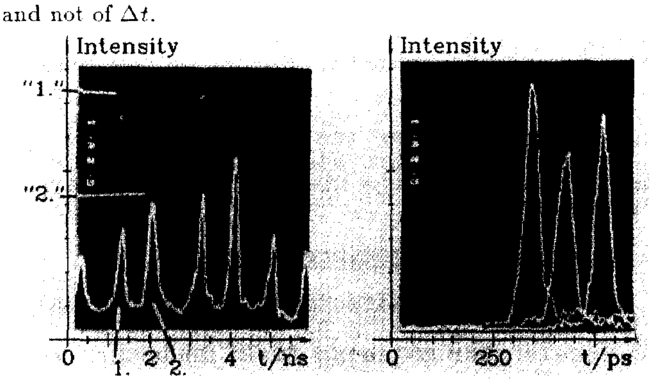

Figure 7: Left: Bunch train measured before (1.) and after (2.) the rotation. Right: (2.) with a higher resolution, showing a $\sigma = 14\,\mathrm{ps}$ for three shots.

The final bunch compression has been studied with the highest resolution of the Čerenkov monitor. With a beam current of $\hat{I} \approx 30\,\mathrm{A}$ and an adjusted phase in the fourth cavity a stable operation with very short bunches of $\sigma = 10$ to $15\,\mathrm{ps}$ has been achieved. Figure 7 (right) shows the second bunch of a bunch train of three consecutive shots. The jitter ($\pm 50\,\mathrm{ps}$) of the trigger electronics has moved the positions within the diagram, so that the pulses can be compared in height and form. With the high energy buncher the bunch length has been compressed by a factor two to three from $\sigma_z \approx 1\,\mathrm{cm}$ to a length of $\sigma_z = 4\,\mathrm{mm}$ to $\sigma_z = 3\,\mathrm{mm}$.

5 Summary and Future Plans

The investigations and measurements at the *Wake Field Transformer* experiment have demonstrated the creation of a hollow driving beam with a diameter of 10 cm, inhomogeneities below 10 % and peak currents of up to 80 A at a gun voltage of 90 kV in a 10 ns long pulse. This pulse is splitt into 5 to 6 bunches 2 ns apart, which are compressed by a prebuncher and a high energy buncher down to a length of $\sigma = 10$ to 15 ps (3–4 mm) with a corresponding high peak current of about 1.5 kA. With these bunch lengths and peak currents the expected gradient for six bunches in the *Wake Field Transformer* is about 20 MeV/m. A test with a 25 cm long transformer section will start this summer.

Acknowledgement

We would like to thank Susan Wipf for carefully reading the manuscript.

References

[1] G.-A.Voss and T.Weiland, *Particle Acceleration by Wake Fields,* DESY M-82-10, April 1982.

[2] G.-A.Voss and T.Weiland, *Wake Field Acceleration Mechanism, Proceedings of the ECFA-RAL Workshop,* Oxford, September 1982, ECFA 83/68 and DESY 82-074 Nov. 1982.

[3] W.Bialowons et al. *A Wake Field Transformer Experiment,* Proceedings of the 12-th International Conference on High Energy Accelerators, Chicago and DESY M-83-27, August 1983.

[4] W.Bialowons et al. *Wake Field Work at DESY,* IEEE Transactions on Nuclear Science, Vol. NS 32-5,2 (1985), pages 3471-3475 and DESY M-85-08.

[5] W.Bialowons et al. *Wake Field Acceleration,* Proceedings of the International Linear Accelerator Conference, SLAC (1986) and Symposium of Advanced Accelerator Concepts, Wisconsin (1986) and DESY M-86-07.

[6] W.Bialowons, H.-D.Bremer, F.-J.Decker, H.-Ch.Lewin, P.Schütt, G.-A.Voss, T.Weiland, Xiao Chengde, *The Wake Field Transformer Experiment at DESY* Proceedings of the ECFA 1987 Workshop in Orsay, France, July 87 or DESY M-87-12.

[7] Franz-Josef Decker, *Zur experimentellen Bestimmung der Dichteverteilung von Elektronenringen am Wake Field Transformator Experiment by DESY,* Thesis, II. Institut für Experimentalphysik der Universität Hamburg, DESY M-87-11, Juli 1987.